Track changes below

The importance of interstitial particle scavenging by cloud droplets in shaping the remote aerosol size distribution and global aerosol-climate effects

J. R. Pierce[1,2], B. Croft[2], J. K. Kodros[1], S. D. D'Andrea[1], R. V. Martin[2],

[1]{Department of Atmospheric Science, Colorado State University, Fort Collins, CO, USA}

[2]{Department of Physics and Atmospheric Science, Dalhousie University, Halifax, NS, Canada}

Correspondence to: J. R. Pierce (jeffrey.pierce@colostate.edu)

Abstract

In this paper, we investigate the coagulation of interstitial aerosol particles (particles too small to activate to cloud droplets) with cloud drops, a process often ignored in aerosol-climate models. We use the GEOS-Chem-TOMAS global chemical transport model with aerosol microphysics to calculate the changes in the aerosol size distribution, cloud-albedo aerosol indirect effect, and direct aerosol effect due to the interstitial coagulation process. We find that inclusion of interstitial coagulation in clouds lowers total particle number concentrations by 15-21% globally, where the range is due to varying assumptions regarding activation diameter, cloud droplet size, and ice cloud physics. The interstitial coagulation process lowers the concentration of particles with dry diameters larger than 80 nm (a proxy for larger CCN) by 10-12%. These 80 nm particles are not directly removed by the interstitial coagulation, but are reduced in concentration because fewer smaller particles grow to diameters larger than 80 nm. The global aerosol indirect effect of adding interstitial coagulation varies from +0.4 to +1.3 W m^{-2} where again the range depends on our cloud assumptions. Thus, the aerosol indirect effect of this process is significant, but the magnitude depends greatly on assumptions regarding activation diameter, cloud droplet size, and ice cloud physics. The aerosol direct effect of interstitial coagulation process is minor (<0.01 W m^{-2}) due to the shift in the aerosol size distribution at sizes where scattering is most effective being small. We recommend that this interstitial scavenging process be considered in aerosol models when the size distribution and aerosol indirect effects are important.

1. Introduction

Atmospheric aerosol particles of both anthropogenic and natural origin have important effects on human health (Dockery et al., 1993), visibility (Malm et al., 2000) and climate (Boucher et al., 2013). The magnitude of these aerosol effects depend on the concentration, composition and size of the particles. The particles may affect climate directly by scattering and absorbing solar radiation (the aerosol direct effect, (Charlson et al., 1992)), and indirectly by acting as cloud condensation nuclei (CCN, the seeds for cloud-droplet formation) and affecting cloud radiative properties (the aerosol

indirect effect, (Twomey, 1974; Albrecht, 1989)). Uncertainties in these aerosol-climate effects are among the leading uncertainties in recent climate forcing changes (Boucher et al., 2013).

The particle size and composition distribution is shaped in the atmosphere by primary emissions of particles, removal of particles through dry and wet deposition, coagulation, aerosol- and cloud-phase chemistry, and condensation from and evaporation to the vapor phase. In remote regions of the atmosphere, away from major anthropogenic sources of particles (e.g. remote oceans and polar regions), understanding the removal processes become increasingly important in simulating aerosol climate effects (Carslaw et al., 2014; Lee et al., 2013; Croft et al., 2014). Lee et al. (2013) shows that uncertainties in dry and wet deposition were ranked first and third, respectively, as the largest contributors to CCN uncertainty in clean remote regions (out 27 uncertain parameters investigated). As aerosol-climate effects are strongly sensitive to CCN concentrations in remote regions due to the low baseline CCN concentrations, particle removal mechanisms must be well represented in aerosol-climate simulations (Carslaw et al., 2013).

Coagulation is an important removal mechanism of particle number, and it moves particle mass towards larger particle sizes. Brownian coagulation, the process where particles collide by diffusion through air, is the dominant coagulation mechanism for aerosol particles (Seinfeld and Pandis, 2006). The coagulation kernel, the rate constant for coagulation between particles of two different sizes, increases as the diameter of the smaller particle decreases (increasing the diffusivity of the smaller particle) and as the larger particle increases (increasing the size of the target for the smaller, diffusing particle). The Brownian coagulation kernel reaches a minimum when the particles have the same size.

In clouds, CCN-sized particles (particles with dry diameters larger than 30-100 nm depending on particle composition and cloud conditions) will activate into cloud droplets, and their diameters will typically grow to 5-20 μm (Rogers and Yau, 1989). The smaller particles will not activate and will continue to have wet diameters below ~100 nm in the cloud. These unactivated particles are referred to as interstitial particles. The increase in size of CCN to cloud droplets will enhance the Brownian coagulation rate between the CCN particles (now cloud droplets) and the interstitial particles. Other effects, such as thermophoresis, diffusiophoresis, turbulence and electrical effects (e.g. charged droplets and/or particles) may also increase the collection of interstitial particles by cloud droplets but are less well understood than Brownian coagulation (Pruppacher and Klett, 1997). Furthermore, if cloud droplets (or ice crystals in ice clouds) grow to diameters beyond ~20 μm, the droplets/crystals will have non-trivial fall speeds relative to the interstitial particles, and gravitational collection of the particles will also contribute to and may dominate coagulation (Rogers and Yau, 1989).

In the case of non-precipitating clouds, the cloud droplets will generally not grow to diameters beyond 20 μm, and Brownian coagulation will dominate the coagulation between droplets and interstitial particles. Any coagulation between the droplets and the interstitial particles will lead to a reduction of interstitial particle number and an increase in the size of the CCN-sized particles after the cloud dries. This coagulation may impact climate in two ways: (1) The removed interstitial particles that may have otherwise grown to CCN sizes via condensation and increased CCN concentrations (Pierce and Adams, 2007; Westervelt et al., 2013; Westervelt et al., 2014). Thus, this coagulation may lower CCN concentrations and lead to a warming through a reduction in the magnitude of the aerosol indirect effect. (2) The shift of particle mass from the smaller, interstitial sizes to the larger sizes of the activated particles may result in a change in the mass scattering and absorption efficiencies of the particles and change the magnitude of the aerosol direct effect (Seinfeld and Pandis, 2006).

In the case of precipitating clouds, the coagulation of particles below clouds by falling drops via gravitational collection directly contributes to wet scavenging/deposition of these particles. The gravitational collection of particles below clouds by precipitation is typically included in global aerosol models and has been investigated in earlier studies of collection efficiency (Greenfield, 1957; Klett and Davis, 1973; Lin and Lee, 1975, Schlamp et al., 1976; Wang et al., 1978; Hall, 1980), parameterizations (Slinn, 1984, Jung and Lee 1997, Croft et al., 2009; Wang et al., 2014) and recent

reviews (Zhang et al., 2013), so we will not focus on these effects in this paper. Brownian coagulation of cloud droplets and interstitial particles still occurs in precipitating clouds, but the collecting cloud droplets will only be wet scavenged/deposited if they are converted into a precipitation drop.

Brownian coagulation of interstitial particles with cloud droplets is often ignored in aerosol models, and we are not aware of any papers that have quantified the importance of this process on aerosol direct and indirect effects on the global scale. Hoose et al. (2008) included Brownian coagulation of interstitial particles with cloud droplets, along with other aerosol-cloud interactions, in the ECHAM-HAM climate model with online aerosol and cloud microphysics. While Hoose et al. (2008) provides zonal mass budgets for how this coagulation impacts the aerosol size modes in their model, they do not explicitly quantify the impact of this coagulation on global aerosol size distributions and climate. The Brownian coagulation of interstitial particles with cloud droplets is also included in the MIRAGE model (Easter et al., 2004; Ghan et al., 2006), but like ECHAM-HAM, we are not aware of a detailed evaluation of this process. Finally, this process is included in HADAM4 (Jones et al., 2001), but this is a mass-only model and does not consider the evolution of the aerosol size distribution. To our knowledge, the Brownian coagulation between interstitial particles and cloud droplets has not previously been considered in many of the other global aerosol microphysics models, including GEOS-Chem-TOMAS (D'Andrea et al., 2013; Pierce et al., 2013; Trivitayanurak et al., 2008), GISS-TOMAS (Adams and Seinfeld, 2002; Pierce and Adams, 2009), GLOMAP (Spracklen et al., 2005~~7~~a,b; 2008, Mann et al., 2012), GLOMAP-Mode (Mann et al., 2010; 2012, Lee et al., 2013), GEOS-Chem-APM (Yu and Luo, 2009; Yu, 2011) and IMPACT (Herzog et al., 2004; Wang and Penner, 2009).

In this paper, we estimate the effects of Brownian coagulation of interstitial particles with cloud droplets in shaping the aerosol size distribution and aerosol-climate effects, globally. Additionally, we compare the simulated size distributions with and without interstitial coagulation to measurements at 21 sites globally to determine if the inclusion of this coagulation improves our simulated size distributions. We only consider Brownian coagulation between the interstitial particles and cloud droplets, and we do not consider thermophoresis, diffusiophoresis, turbulence, or electrical effects. These other effects will change the rate of coagulation of the interstitial particles in the accumulation mode size range with the cloud droplets, and will have less influence on the smaller particles relative to the effects of Brownian diffusion. In the following section, we describe the GEOS-Chem-TOMAS global chemical transport model with online aerosol microphysics used in this study, the modifications we made to the model, and the various model simulations. In Section 3, we provide the results and analysis of our model simulations estimating the effect of interstitial particle coagulation by cloud droplets, and we compare our simulated results to measurements. Finally, we provide conclusions in Section 4.

2. Methods

2.1. GEOS-Chem-TOMAS overview

In this paper, we simulate global aerosol size distributions using the GEOS-Chem-TOMAS model, which is a coupling of the GEOS-Chem global chemical transport model (www.geos-chem.org, Bey et al., 2001) with the TwO-Moment Aerosol Sectional (TOMAS) microphysics scheme (Adams and Seinfeld, 2002; Lee and Adams, 2012). In this work, model simulations use GEOS-Chem version 9.02 at 4°x5° resolution globally with 47 layers extending from the surface to 0.01 hPa. Modelled meteorology is taken from the National Aeronautics and Space Administration (NASA) Global Modelling and Assimilation Office (GMAO) Goddard Earth Observing System version 5 (GEOS-5) assimilated meteorology product. All simulations are use year 2012 meteorology and emissions

following a 3 month spin-up at the end of 2011. GEOS-Chem includes simulation of 50 gas-phase species including aerosol precursor gases such as SO_2 and NH_3.

TOMAS in this work tracks the number and mass of particles within each of 15 size sections. The first 13 size sections are logarithmically spaced and span diameters from approximately 3 nm to 1 μm, and the 2 final size sections span 1 μm to 10 μm (Lee and Adams, 2012). Particle composition includes sulfate, ammonia, sea-spray, hydrophilic organics, hydrophobic organics, internally mixed black carbon, externally mixed black carbon, dust and water. Particle nucleation is estimated using the ternary scheme (H_2SO_4+NH_3+H_2O) of Napari et al. (2002) with nucleation rates scaled by 10^{-5}, which showed good agreement versus observation in Westervelt et al. (2013), and the binary (H_2SO_4+H_2O) nucleation scheme of Vehkamaki et al. (2012) in the regions with NH_3 mixing ratios below the Napari et al. (2002) threshold. Particle sizes below 3 nm are approximated using the Kerminen et al. (2004) scheme, which has been evaluated in TOMAS in Lee et al. (2013). Secondary organic aerosol (SOA) includes both a biogenic contribution and an anthropogenic (or anthropogenically enhanced yields of biogenic SOA)) contribution and is considered to be non-volatile for the condensation parameterization as in D'Andrea et al. (2013). Emissions in GEOS-Chem-TOMAS are described in detail in Stevens and Pierce (2014).

Coagulation between particles in GEOS-Chem-TOMAS occurs using the Brownian coagulation scheme of Fuchs (1964). Prior to this work, the particle size for the coagulation parameterization was found using the grid-box-mean relative humidity for water uptake (capped at 99%) both in and out of clouds. Thus in clouds, previous versions did not account for Brownian coagulation of interstitial aerosols with particles that have grown to cloud droplet size. This previous model version that lacked coagulation between interstitial particles and cloud droplets will be our base assumption for comparison in this paper.

2.2. Brownian coagulation between interstitial particles with cloud droplets

In this work, we add Brownian coagulation between interstitial particles and particles that are assumed to have activated and grown to cloud droplet size. In the GEOS-5 assimilated meteorological fields, model grid boxes are divided into cloudy fractions and non-cloudy fractions. For the cloudy fraction of the grid box, we assume that all particles above a certain size threshold activated into cloud droplets (this size threshold is varied in different simulations described below). We assume that the activated aerosols have a fixed wet size equal to the assumed cloud droplet size, which is varied between simulations, described below. The coagulation kernel is then calculated between all particle size-bin combinations regardless of whether the particles in the bin are activated or not. Similarly, we calculate the coagulation kernel for the non-cloudy portion of the grid box for all size-bin combinations assuming that all bins are of non-activated wet size. The grid-box-mean coagulation rate between any two size bins is then calculated as follows:

$$J_{i,j} = (1 - f_{cloudy}) K_{clear;i,j} N_i N_j + f_{cloudy} K_{cloudy;i,j} N_i N_j \quad \text{Eqn. 1}$$

where $J_{i,j}$ is the coagulation rate between particles in bins i and bin j, f_{cloudy} is the fraction of the grid box that is cloudy, $K_{clear;i,j}$ is the coagulation kernel between bins i and j in the clear portion of the gridbox, $K_{cloudy;i,j}$ is the coagulation kernel between bins i and j in the cloudy portion of the gridbox, N_i is the number concentration of particles in bin i, and N_j is the number concentration of particles in bin j.

In our base simulations for comparison, we do not consider Brownian coagulation between interstitial particles and cloud droplets, which is equivalent to assuming the f_{cloudy} is 0 in Eqn. 1. $K_{cloudy;i,j}$ is determined by the size of the interstitial and activated particles, which we vary between sensitivity simulations and are discussed next. We apply this interstitial coagulation mechanism only when temperatures are above 238K (threshold for homogeneous freezing, (Koop et al., 2000)) because the crystal size distributions and concentrations in ice clouds are much more variable than those of liquid clouds. As glaciation often occurs at warmer temperatures, we perform a sensitivity simulation to this

temperature cutoff, described below. We justify this temperature threshold since super-cooled liquid clouds can exist at temperatures as cold as 238K, although the onset of glaciation can occur at temperatures as warm as 258-263K (Rosenfeld and Woodley, 2000, Rosenfeld et al., 2011). Recent studies indicate that low-level liquid clouds are ubiquitous in all seasons in remote regions such as the Arctic (e.g. Cesana et al., 2012). Thus, we also perform a simulation where we limit interstitial coagulation to temperatures warmer than 258K.

2.3. Simulations

Table 1 summarises the simulations performed for this paper. As stated earlier, in our BASE simulation there is no interstitial coagulation by aerosols of cloud droplet size, and the coagulation scheme for the entire gridbox assumes all particles are of non-activated size ($K_{clear;i,j}$). In the INT_65nm_10μm_238K simulation, all particles with dry diameters larger than 65nm in the cloudy fraction of gridboxes warmer than 238 K are assumed to have wet diameters of 10 μm (i.e. the critical diameter for activation is 65 nm, and the cloud droplet diameter is 10 μm for all droplets). $K_{cloudy;i,j}$ is calculated using this new wet diameter for the particles with dry diameters larger than the critical 65 nm value. Thus, the coagulation rate between any two particles, both with dry diameters smaller than 65 nm, remains unchanged from the clear-sky value. For clouds colder than 238 K, we do not consider interstitial coagulation. We test the sensitivity of our results of this temperature cutoff as well as the critical activation dry diameter and the assumed cloud droplet diameter. In the INT_65nm_13μm_238K simulation, particles in the cloudy fraction of the gridbox with dry diameters larger than 65 nm are assumed to have wet diameters of 13 μm. In the INT_40nm_10μm_238K simulation, particles in the cloudy fraction of the gridbox with dry diameters larger than 40 nm are assumed to have wet diameters of 10 μm. Finally, in the INT_65nm_10μm_258K simulation, interstitial scavenging is only considered in clouds warmer than 258 K.

None of these simulations capture the variability in clouds throughout the globe (e.g. minimum activation diameters, cloud droplet sizes, glaciation temperatures); however, in this work, we are attempting to bound the aerosol and climate effects of interstitial scavenging that are frequently overlooked in aerosol simulations.

2.4. Radiative forcing calculations

The direct radiative effect (DRE) is calculated using the parameterization of Chylek and Wong (1995), which uses the single-scatter approximation. Optical properties for aerosols are calculated from monthly averaged GEOS-Chem-TOMAS aerosol number and mass size distributions with refractive indices for each aerosol species from the Global Aerosol Database (GADs) (Koepke et al. 1997; d'Almedia et al. 1991). We calculate the direct radiative effect assuming the particles are internally mixed, and scattering species (e.g. sulfate and organics) form a shell around black carbon (core-shell assumption). We volume weight the refractive index of the scattering species. Scattering and absorption efficiencies and the asymmetry parameter were calculated using the Bohren and Huffman (1983) coated sphere mie code ('BHCOAT'). Surface albedo and cloud fraction are taken as monthly averages from GEOS5. We assume no aerosol effects in cloudy columns, and our all-sky DRE is the clear-sky DRE multiplied by the clear-sky fraction.

We calculate the cloud-albedo aerosol indirect effect (AIE) offline by calculating a change in monthly averaged cloud reflectivity due to a change in monthly average aerosol number and mass size distributions. We calculate the number of activated particles for each simulation using the Abdul-Razzak and Ghan activation parameterization (Abdul-Razzak et al., 2002) and assuming a constant updraft velocity of 0.2 m s^{-1}. Cloud optical depth is then calculated using monthly averaged activated particle concentrations, and the monthly averaged liquid water content in the mean cloudy fraction of each grid box from the GEOS5 met fields. Cloud reflectivity is calculated from the cloud optical depth using the two-stream approximation assuming a non-absorbing, horizontally homogenous

cloud (Lacis and Hansen, 1974), which may lead to an overprediction of cloud albedo of as much as 10% (Oreopoulis et al., 2007). The change in cloud albedo forcing for two simulations is then the product of the change in total albedo, incoming solar radiation, cloud area, surface albedo, and atmospheric transmittance (Lacis and Hansen, 1974).

While both our DRE and AIE calculations include simplifying assumptions (e.g. monthly mean aerosol and cloud fields, a single-scatter approximation for DRE, and no DRE in cloudy columns), these calculations should be sufficient for determining the general range of DRE and AIE changes that are expected from inclusion of coagulation of interstitial particles by cloud droplets. These simplified calculations allow us to determine if the interstitial scavenging is important in shaping radiative effects.

3. Results

3.1. Sensitivity of aerosols and radiative forcing to interstitial scavenging

Table 2 shows the global-2km-altitude- and annual-mean relative changes in N10 and N80 (the number concentration of particles larger than 10 and 80 nm, respectively) and absolute changes of the AIE between the various interstitial-scavenging simulations and BASE simulation. The 2 km layer is shown here as being representative of low-level clouds. The global-mean changes in N10 and N80 are -18.4% and -10.2%, respectively, between INT_65nm_10μm_238K and BASE. Thus, not only are particles with dry diameters smaller than the 65 nm activation cutoff being reduced in concentration due to interstitial scavenging, particles larger than this (e.g. N80) are also being reduced in concentration. In clouds, the coagulation rate between the particles with diameters larger than 65 nm would be slower than outside of the cloud because we only consider Brownian coagulation and we assume all cloud droplets have the same diameter (uniform sizes leads to reduced coagulation rates compared to polydisperse sizes). Thus, the reduction in N80 is due to a reduction of the number of particles with dry diameters smaller than 65 nm and a subsequent reduction of the number of particles growing from these smaller sizes to 80 nm through condensation growth.

Figure 1 shows the spatial patterns of annual-mean changes in N10 and N80 between the INT_65nm_10μm_238K simulation and the BASE simulation. Figure 1a shows the change in N10 in the 2 km layer of the model (to represent the boundary layer). The largest changes are in remote regions with low aerosol source strengths (e.g. the Arctic and extratropical oceans) where the reductions in N10 exceed 25%. There are some regions with little (<1%) change in N10. These are generally in regions of low cloud-cover amount that are downwind of cloudier regions. There is enhanced nucleation in these low cloud-cover-amount regions due to a lower condensation sink advecting in from cloudier regions upwind. Figure 1c shows that the zonal changes in N10 are larger than 10% throughout nearly all of the troposphere. Figure 1b shows the 2 km changes in N80. N80 are reduced by over 1% over the entire 2 km layer due to interstitial scavenging, and are greater than 5% in regions outside of the tropical continental regions. Decreases exceed 10% in remote midlatitude and polar regions. The decreases in the Arctic exceed 20%. Figure 1d shows that the decreases in N80 due to interstitial scavenging are generally between 10-20% in the free troposphere. These decreases in remote regions show that away from sources, the effects of interstitial scavenging on CCN-sized might have significant climatic effects.

Figure 2 shows the predicted annual-mean AIE between the INT_65nm_10μm_238K simulation and the BASE simulation. The global mean AIE of interstitial scavenging (Table 2) is +1.02 W m^{-2} between these simulations showing that the interstitial scavenging causes a reduction in the amount of cooling of the AIE. The AIE of interstitial scavenging is over +1 W m^{-2} throughout most tropical and midlatitude oceanic regions and over +1.5 W m^{-2} throughout much of the northern hemisphere oceans. There are regions of smaller AIE of interstitial scavenging over continents due to different combinations of (1) bright surfaces (e.g. northern Africa, Middle East, Australia), (2) lower

cloud-cover amounts (same regions), and (3) very high CCN concentrations saturating AIE changes (e.g. China, eastern North America, Europe, southern Africa).

We also calculated the direct radiative effect (DRE) between the INT_65nm_10μm_238K simulation and the BASE simulation. The global mean DRE was cooling, but smaller in magnitude than -0.01 W m^{-2} for all interstitial scavenging simulations relative to the BASE simulation (not shown due to the small magnitude). The slight cooling was due to a shift in the aerosol mass distribution towards slightly larger sizes due to the enhanced coagulation between the ultrafine particles and the activated particles in clouds. These larger sizes are closer to the peak size of the mass scattering efficiency, and thus there is a net negative DRE between the simulations with interstitial scavenging and the BASE simulation (there was also a enhancement in absorption due to the shift in size, but in smaller magnitude to the scattering effect). While there was a large change in N80 number concentrations, which greatly affected the AIE, the DRE was largely insensitive to the interstitial scavenging because the changes in mass and mass-scatter/absorption efficiencies were small.

Table 2 also shows the global-mean N10, N80 and AIE changes of the interstitial scavenging sensitivity studies versus BASE. We do not show maps for each of these sensitivity cases because the spatial patterns are qualitatively similar to Figures 2 and 3. Increasing the diameter of the cloud droplets to 13 μm (INT_65nm_13μm_238K) leads to ~10-20% strengthening of the decreases in N10 and N80 and a 15% strengthening of the increase in AIE difference relative to the case with 10 μm cloud droplets. This strengthening of the interstitial scavenging effects is due to enhanced Brownian coagulation rates because of the larger cloud droplets.

Decreasing the activation cutoff diameter to 40 nm (INT_40nm_10μm_238K) leads to enhanced reduction of N10 relative to the 65 nm cutoff at the same temperature threshold and cloud droplet size (-20.8% rather than -18.4%); however, the reduction in N80 is similar to the 65 nm cutoff (-10.9% rather than -10.2%). The 40 nm cutoff means that more particles will activate and participate as scavengers than compared to the simulations with the 65 nm cutoff; however, the 40-65 nm particles no longer undergo enhanced scavenging. The AIE for the 40 nm cutoff diameter is about 20% stronger than in the 65 nm cutoff case because in many remote locations particles smaller than 80 nm activate in our AIE calculation.

Increasing the glaciation temperature to 258 K from 238 K (INT_65nm_10μm_258K) reduces the effects of the interstitial scavenging because fewer clouds included the interstitial scavenging in the simulation, particularly at high latitudes and altitudes. The magnitude of the AIE for the 258 K case is roughly half of the AIE from the 238 K case. Thus, the uncertainties in interstitial scavenging in ice clouds, which we ignore here, as well as the temperature at which clouds glaciate, contribute large uncertainties to the strength of interstitial scavenging effects.

Overall, our sensitivity studies show that the interstitial scavenging of particles by cloud drops may reduce aerosol number concentrations by about 10-20% and decrease the amount of cloud cooling (AIE) by about 1 W m^{-2}; however, these magnitudes are uncertain on the order of a factor of 2 due to uncertainties or variability in activation diameter, cloud droplet size, and ice cloud physics.

3.2. Comparisons to aerosol size-distribution observations

In this section, we compare our simulations to aerosol size-distribution measurements to determine how the addition of interstitial scavenging changes model performance. These results should be viewed with caution because aerosol microphysics models may have cancelingcancelling errors, and improved results may occur for wrong reasons. Nonetheless, this comparison shows how the current state of the model changes relative to observations with the addition of new physics.

For the comparisons, we use long-term (1 year or longer) aerosol size distribution observations from 21 field sites. These data are described in detail in D'Andrea et al. (2013) with a map of the locations in Figure 1 of that study. The measurements at these sites were from either Scanning Mobility Particle Sizers (SMPSs) or Differential Mobility Particle Sizers (DMPSs).

Figure 3 shows the annual-mean size distributions at each location for the measurements and the model for the BASE and INT_65nm_10μm_238K simulations. The inclusion of interstitial coagulation decreases the number of sub-100nm particles at many remote locations. Figure 43 shows comparisons of modelled to measured annual-mean N10, N40, N80 and N150 at the 21 sites for each of the 5 simulations. The statistics of the comparisons are given in Table 3. The statistics are log-mean bias (LMB), slope (m), and coefficient of determination (R^2). We use the coefficient of determination rather than the correlation coefficient (R) because the coefficient of determination quantifies the fraction of the variance in the measurements that is captured by the model. Including interstitial scavenging improves the slope of the comparison of N10, N40 and N80 to measurements for all 4 interstitial scavenging simulations relative to the BASE simulation. The predicted concentration of N10, N40 and N80 in clean regions was, on average, too high in the base simulation, and the interstitial scavenging corrects this to some degree. The INT_65nm_13μm_238K simulation, which had the most aggressive interstitial scavenging, had the best slopes for N10, N40 and N80, so it is possible that increasing the rate of interstitial scavenging beyond that of this simulation may further improve the slopes. The slope of the N150 relative to measurements does not change because particles with diameters larger than 150 nm were less affected by the addition of interstitial scavenging than smaller particles (fewer particles grow to 150 nm than grow to 80 nm).

The inclusion of interstitial scavenging lowers the mean predicted values of N10, N40, N80 and N150, which means that the LMB has more negative values for the interstitial scavenging simulations relative to BASE. Whether or not interstitial scavenging improves the LMB depends on the LMB of the BASE simulation. The LMB for N10 and N150 in the BASE simulation are positive, and the inclusion of interstitial scavenging brings the LMB to values closer to zero. For N40 and N80, the inclusion of interstitial scavenging brings the LMB to negative values that are further from zero than the BASE simulation. Thus, the inclusion of interstitial scavenging brings the LMB to more negative values, but neither shows a clear improvement or deterioration compared to the BASE simulation. Finally, the inclusion of interstitial scavenging does little to change the scatter across the various sites, so the R^2 values do not change greatly.

In summary, the inclusion of interstitial scavenging improves the slope of N10, N40 and N80 comparisons to observations but has little effect on the slope of N150 and the LMB and R^2 of all sizes. Again, the improvement of the slopes shown here could be due to interstitial scavenging cancelling errors from elsewhere in the model; however, because interstitial scavenging is a physical processes that was lacking in our model previously, it is encouraging that the model performance improved through its inclusion.

4. Conclusions

In this paper, we test the sensitivity of the global aerosol size distributions and radiative forcing to the scavenging of interstitial aerosol particles by cloud droplets. We limit this study to scavenging in liquid clouds. We make simple assumptions about cloud droplet activation and the size of the cloud droplets as a starting point for understanding the impact of interstitial scavenging. The inclusion of interstitial scavenging was found to decrease the total number of particles larger than 10 nm (N10) by 15-21% at 2 km, relative to a simulation with no interstitial scavenging. The range was due to different simulations where we changed the cutoff temperature for ice clouds, the minimum aerosol activation diameter, and the cloud droplet diameter. The number of particles larger than 80 nm (N80, a proxy for CCN) decreased by 10-12% at 2 km even though particles of this size were not directly removed by the interstitial scavenging. N80 was reduced when interstitial scavenging was included because of fewer particles grew to 80 nm diameters from smaller sizes. The global-mean aerosol indirect effect of including interstitial scavenging was +0.5 to +1.3 W m^{-2}, but the aerosol direct effect of this process was negligible (~-0.01 W m^{-2}) because neither the total mass nor the mass-scatter/absorption efficiencies changed.

While the simulations in this paper use simplified assumptions regarding the critical aerosol activation diameter and diameter of cloud droplets, our sensitivity tests show that the scavenging of interstitial particles by cloud droplets yields important (>10%) changes in the aerosol size distribution, particularly in remote regions away from sources. These changes provided an improvement in comparison of the simulated aerosol size distribution to SMPS/DMPS measurements at 21 global sites; however, we acknowledge that these improvements could be due to a cancelling of other errors in the model. We only consider Brownian coagulation between the interstitial particles and cloud droplets, and we do not consider thermophoresis, diffusiophoresis, turbulence, electrical effects. These effects are expected to be less important for collection of particles at the size range of the interstitial aerosols.

Thus, while the scavenging of interstitial particles by cloud droplets has often been left out of previous aerosol-climate studies, we recommend aerosol microphysics models include this process since the effects on aerosols and climate are substantial in many global regions. Interstitial scavenging has aerosol-climate effects of similar magnitude as uncertainties in nucleation (Merikanto et al., 2009; Pierce and Adams, 2009a; Reddington et al., 2011; Spracklen et al., 2008; Wang and Penner, 2009), primary emissions (Adams and Seinfeld, 2003; Pierce and Adams, 2006, 2009; Reddington et al., 2011; Spracklen et al., 2011), wet/dry deposition (Croft et al., 2012) and other factors (Lee et al., 2013); hence, since significant effort is put into improving these other processes in models, we recommend attention be paid to the coagulation of interstitial particles by cloud droplets. Our simple methods here may be further refined by including online schemes that calculate aerosol activation from updraft velocities and the aerosol size distribution (e.g. Nenes and Seinfeld, (2003); Abdul-Razzak and Ghan (2000)). The MIRAGE and ECHAM-HAM models (Herzog et al., 2004; Ghan et al., 2006; Hoose et al., 2008) already include these online activations schemes as well as the interstitial coagulation described here, so these models may be seen as state-of-the-art for this process.

5. Acknowledgements

The authors acknowledge Natural Sciences and Engineering Research Council (NSERC) of Canada for funding through the Network on Climate and Aerosols (NETCARE) network. We thank the Atlantic Computational Excellence Network (ACENet) for the computational resources used in this study.

6. References

Abdul-Razzak, H. and Ghan, S. J.: A parameterization of aerosol activation: 2. Multiple aerosol types, J. Geophys. Res., 105, 6837, doi:10.1029/1999JD901161, 2000.

Adams, P. J. and Seinfeld, J. H.: Predicting global aerosol size distributions in general circulation models, J. Geophys. Res., 107(D19), 4310–4370, 2002.

Adams, P. J. and Seinfeld, J. H.: Disproportionate impact of particulate emissions on global cloud condensation nuclei concentrations, Geophys. Res. Lett., 30(5), 1210–1239, 2003.

Albrecht, B. A.: Aerosols, Cloud Microphysics, and Fractional Cloudiness, Science, 245(4923), 1227–1230, 1989.

Bohren, C. F. and Huffman, D. R., Appendix B: Coated Sphere, in Absorption and Scattering of Light by Small Particles, Wiley-VCH Verlag GmbH, Weinheim, Germany. doi: 10.1002/9783527618156.app3, 1998.

Boucher, O., D. Randall, P. Artaxo, C. Bretherton, G. Feingold, P. Forster, V.-M. Kerminen, Y. Kondo, H. Liao, U. and Lohmann, P. Rasch, S.K. Satheesh, S. Sherwood, B. Stevens, X. Y. Z.: Clouds and

Aerosols, in Climate Change 2013: The Physical Science Basis. Contribution of Working Group I to the Fifth Assessment Report of the Intergovernmental Panel on Climate Change, edited by J. B. Stocker, T.F., D. Qin, G.-K. Plattner, M. Tignor, S.K. Allen and P. M. M. A. Nauels, Y. Xia, V. Bex, Cambridge University Press, Cambridge, United Kingdom and New York, NY, USA., 2013.

Carslaw, K. S., Lee, L. A, Reddington, C. L., Pringle, K. J., Rap, A, Forster, P. M., Mann, G. W., Spracklen, D. V, Woodhouse, M. T., Regayre, L. A and Pierce, J. R.: Large contribution of natural aerosols to uncertainty in indirect forcing., Nature, 503, 67–71, doi:10.1038/nature12674, 2013.

Charlson, R. J., Schwartz, S. E., Hales, J. M., Cess, R. D., Coakley, J. A., Hansen, J. E. and Hofman, D. J.: Climate Forcing by Anthropogenic Aerosols, Science., 255(5043), 423–430, 1992.

Chylek, P. and Wong, J.: Effect of absorbing aerosols on global radiation budget, Geophys. Res. Lett., 22(8), 929–931, 1995.

Croft, B., Lohmann, U., Martin, R. V., Stier, P., Wurzler, S., Feichter, J., Posselt, R., and Ferrachat, S.: Aerosol size-dependent below-cloud scavenging by rain and snow in the ECHAM5-HAM, Atmos. Chem. Phys., 9, 4653–4675, 2009, http://www.atmos-chem-phys.net/9/4653/2009/.

Croft, B., Pierce, J. R., Martin, R. V., Hoose, C. and Lohmann, U.: Uncertainty associated with convective wet removal of entrained aerosols in a global climate model, Atmos. Chem. Phys., 12(22), 10725–10748, doi:10.5194/acp-12-10725-2012, 2012.

Croft, B., Pierce, J. R., and Martin, R. V.: Interpreting aerosol lifetimes using the GEOS-Chem model and constraints from radionuclide measurements, Atmos. Chem. Phys., 14, 4313-4325, doi:10.5194/acp-14-4313-2014, 2014.

d'Almedia, G.A., P. Koepke, and E.P. Shettle: Atmospheric Aerosols: Global Climatology and Radiative Characteristics, A. Deepak Publishing, 561 pp., 1991.

D'Andrea, S. D., Hakkinen, S. A. K., Westervelt, D. M., Kuang, C., Levin, E. J. T., Kanawade, V. P., Leaitch, W. R., Spracklen, D. V., Riipinen, I., and Pierce, J. R.: Understanding global secondary organic aerosol amount and size-resolved condensational behavior, Atmos. Chem. Phys., 13, 11519-11534, doi:10.5194/acp-13-11519-11534, 2013.

Dockery, D. W., Pope, C. A., Xu, X., Spengler, J. D., Ware, J. H., Fay, M. E., Ferris, B. G. and Speizer, F. E.: An association between air pollution and mortality in six U.S. cities., N. Engl. J. Med., 329, 1753–1759, doi:10.1097/00043764-199502000-00008, 1993.

Easter, R. C., Ghan, S. J., Zhang, Y., Saylor, R. D., Chapman, E. G., Laulainen, N. S., Abdul-Razzak, H., Leung, L. R., Bian, X. D. and Zaveri, R. A.: MIRAGE: Model description and evaluation of aerosols and trace gases, J. Geophys. Res., 109(D20), -20210, 2004.

Fuchs, N. A.: Mechanics of Aerosols, Pergamon, New York., 1964.

Gong, S. L., Barrie, L. A., and Blanchet, J.-P.: Modeling sea-salt aerosols in the atmosphere: 1. Model development, J. Geophys. Res., 102, 3805–3818, 1997.

Ghan, S. J., Rissman, T. A., Elleman, R., Ferrare, R. A., Turner, D., Flynn, C., Wang, J., Ogren, J., Hudson, J., Jonsson, H. H., VanReken, T., Flagan, R. C. and Seinfeld, J. H.: Use of in situ cloud condensation nuclei, extinction, and aerosol size distribution measurements to test a method for retrieving cloud condensation nuclei profiles from surface measurements, J. Geophys. Res., 111(D5), 2006.

Greenfield, S.: Rain scavenging of radioactive particulate matter from the atmosphere., J. Meteor., 14, 115–125, 1957.

Hall, W. D.: A detailed microphysical model within a two-dimensional dynamic framework:Model description and preliminary results., J. Atmos. Sci., 37, 2486–2507, 1980.

Henzing, J. S., Olivie, D. J. L., and Velthoven, P. F. J. V.: A parameterization of size resolved below cloud scavenging of aerosols by rain, Atmos. Chem. Phys., 6, 3363–3375, 2006, http://www.atmos-chem-phys.net/6/3363/2006/.

Herzog, M., Weisenstein, D. K. and Penner, J. E.: A dynamic aerosol module for global chemical transport models: Model description, J. Geophys. Res. Atmos., 109, doi:10.1029/2003JD004405, 2004.

Hoose, C., Lohmann, U., Bennartz, R., Croft, B. and Lesins, G.: Global simulations of aerosol processing in clouds, Atmos. Chem. Phys. Discuss., 8(4), 13555–13618, 2008.

Koepke P., M. Hess, I. Schult, and E.P. Shettle, "Global aerosol dataset", Report N 243, Max-Plank-Institut für Meteorologie, Hamburg, 44 pp., September 1997.

Jones, A., Roberts, D. L., Woodage, M. J. and Johnson, C. E.: Indirect sulphate aerosol forcing in a climate model with an interactive sulphur cycle, J. Geophys. Res., 106(D17), 20293–20310, 2001.

Jung, C. H. and Lee, K. W.: Filtration of fine particles by multiple liquid drop and gas bubble systems, Aeros. Sci. Tech., 29, 389–401, 1998.

Kärcher, B. and and Lohmann, U.: A parameterization of cirrus cloud formation: Homogeneous freezing of supercooled aerosols, J. Geophys. Res., 107(D2), 4010, doi:10.1029/2001JD000470,2002.

Kerminen, V. M., Anttila, T., Lehtinen, K. E. J. and Kulmala, M.: Parameterization for atmospheric new-particle formation: Application to a system involving sulfuric acid and condensable water-soluble organic vapors, Aerosol Sci. Technol., 38(10), 1001–1008, 2004.

Klett, J. D. and Davis, M. H.: Theoretical collision efficiencies of cloud droplets at small Reynolds numbers, J. Atmos. Sci., 30, 107–117, 1973.

Koop, T., Luo, B., Tsias, A. and Peter, T.: Water activity as the determinant for homogeneous ice nucleation in aqueous solutions, , (1), 611–614, 2000.

Lacis, A. A. and Hansen, J.: A Parameterization for the Absorption of Solar Radiation in the Earth's Atmosphere, J. Atmos. Sci., 31, 118–133, doi:10.1175/1520-0469, 1974.

Lee, L. A., Pringle, K. J., Reddington, C. L., Mann, G. W., Stier, P., Spracklen, D. V., Pierce, J. R. and Carslaw, K. S.: The magnitude and causes of uncertainty in global model simulations of cloud condensation nuclei, Atmos. Chem. Phys., 13(17), 8879–8914, doi:10.5194/acpd-13-6295-2013, 2013.

Lee, Y. H. and Adams, P. J.: A Fast and Efficient Version of the TwO-Moment Aerosol Sectional (TOMAS) Global Aerosol Microphysics Model, Aerosol Sci. Technol., 46(6), 678–689, doi:10.1080/02786826.2011.643259, 2012.

Lee, Y.H., Pierce, J.R., Adams, P.J.: Representation of nucleation mode microphysics in global aerosol microphysics models, Geosci. Model Dev., 6, 1221-1232, doi:10.5194/gmd-6-1221-2013, 2013.

Lin, C. L. and Lee, S.: Collision efficiency of water drops in the atmosphere., J. Atmos. Sci., 32, 1412–1418, 1975

Malm, W. C., Pitchford, M. L., Scruggs, M., Sisler, J. F., Ames, R., Copeland, S., Gebhart, K. A. and Day, D. E.: Spational and Seasonal Patterns and Temporal Variability of Haze and its Constituents in the United States: Report III, Coop. Inst. for Res., Colo. State Univ., 2000.

Mann, G. W., Carslaw, K. S., Spracklen, D. V., Ridley, D. A., Manktelow, P. T., Chipperfield, M. P., Pickering, S. J. and Johnson, C. E.: Description and evaluation of GLOMAP-mode: a modal global aerosol microphysics model for the UKCA composition-climate model, Geosci. Model Dev. Discuss., 3, 651–734, doi:10.5194/gmdd-3-651-2010, 2010.

Mann, G. W., Carslaw, K. S., Ridley, D. A., Spracklen, D. V., Pringle, K. J., Merikanto, J., Korhonen, H., Schwarz, J. P., Lee, L. A., Manktelow, P. T., Woodhouse, M. T., Schmidt, A., Breider, T. J., Emmerson, K. M., Reddington, C. L., Chipperfield, M. P. and Pickering, S. J.: Intercomparison of modal and sectional aerosol microphysics representations within the same 3-D global chemical transport model, Atmos. Chem. Phys., 12, 4449–4476, doi:10.5194/acp-12-4449-2012, 2012.

Merikanto, J., Spracklen, D., Mann, G. W., Pickering, S. J. and Carslaw, K. S.: Impact of nucleation on global CCN, Atmos. Chem. Phys., 9, 8601–8616, 2009.

Napari, I., Noppel, M., Vehkamaki, H. and Kulmala, M.: Parametrization of ternary nucleation rates for H2SO4-NH3-H2O vapors, J. Geophys. Res., 107(D19), 4310–4381, 2002.

Nenes, A. and Seinfeld, J. H.: Parameterization of cloud droplet formation in global climate models, J. Geophys. Res., 108(D14), 4415, doi:10.1029/2002JD002911, 2003.

Oreopoulis, L., Cahalan, R.F., Platnick, S.: The Plane-Parallel Albedo Bias of Liquid Clouds from MODIS Observations, J. Climate, 20, 5114-5125, DOI: 10.1175/JCLI4305.1, 2007.

Pierce, J. R. and Adams, P. J.: Global evaluation of CCN formation by direct emission of sea salt and growth of ultrafine sea salt, J. Geophys. Res., 111(D6), D06203, doi:10.1029/2005JD006186, 2006.

Pierce, J. R. and Adams, P. J.: Efficiency of cloud condensation nuclei formation from ultrafine particles, Atmos. Chem. Phys., 7, 1367–1379, 2007.

Pierce, J.R., Adams, P.J., Uncertainty in global CCN concentrations from uncertain aerosol nucleation and primary emission rates, Atmospheric Chemistry and Physics, 9, 1339-1356, 2009.

Pierce, J.R., Evans, M.J., Scott, C.E., D'Andrea, S.D., Farmer, D.K., Swietlicki, E., Spracklen, D.V.: Weak sensitivity of cloud condensation nuclei and the aerosol indirect effect to Criegee+SO2 chemistry, Atmospheric Chemistry and Physics, 13, 3163-3176, doi:10.5194/acp-13-3163-2013, 2013.

Pruppacher, H. R. and Klett, J. D.: Microphysics of Clouds and Precipitation, 2nd ed., Kluwer Academic Publishers, Dordrecht, The Netherlands., 1997.

Reddington, C. L., Carslaw, K. S., Spracklen, D. V., Frontoso, M. G., Collins, L., Merikanto, J., Minikin, a., Hamburger, T., Coe, H., Kulmala, M., Aalto, P., Flentje, H., Plass-Dülmer, C., Birmili, W., Wiedensohler, a., Wehner, B., Tuch, T., Sonntag, a., O'Dowd, C. D., Jennings, S. G., Dupuy, R., Baltensperger, U., Weingartner, E., Hansson, H.-C., Tunved, P., Laj, P., Sellegri, K., Boulon, J., Putaud, J.-P., Gruening, C., Swietlicki, E., Roldin, P., Henzing, J. S., Moerman, M., Mihalopoulos, N., Kouvarakis, G., Ždímal, V., Zíková, N., Marinoni, a., Bonasoni, P. and Duchi, R.: Primary versus secondary contributions to particle number concentrations in the European boundary layer, Atmos. Chem. Phys., 11(23), 12007–12036, doi:10.5194/acp-11-12007-2011, 2011.

Rogers, R. R. and Yau, M. K.: A Short Course in Cloud Physics, 3rd ed., Butterworth-Heinmann, Oxford, UK., 1989.

Rosenfeld, D. and Woodley, W. L.: Deep convective clouds with sustained supercooled liquid water down to - 37.5°C, 405, 23–25, 2000.

Rosenfeld, D., Yu, X., Liu, G., Xu, X., Zhu, Y., Yue, Z., Dai, J., Dong, Z., Dong, Y. and Peng, Y.: Glaciation temperatures of convective clouds ingesting desert dust, air pollution and smoke from forest fires, Geophys. Res. Lett., 38(21), doi:10.1029/2011GL049423, 2011.

Seinfeld, J. H. and Pandis, S. N.: Atmospheric Chemistry and Physics, 1st ed., John Wiley and Sons., New York., 2006.

Schlamp, R. J., Grover, S. N., and Pruppacher, H. R.: A numerical investigation of the effect of electric charges and vertical external electric fields on the collision efficiency of cloud drops., J. Atmos. Sci., 33, 1747–1755, 1976

Slinn, W. G. N.: Precipitation Scavenging in Atmospheric Science and Power Production, CH. 11, edited by: Randerson, D., Tech. Inf. Cent., Off. of Sci. and Techn. Inf., Dep. of Energy, Washington DC, USA, 466–532, 1984.

Spracklen, D. V, Pringle, K. J., Carslaw, K. S., Chipperfield, M. P. and Mann, G. W.: A global off-line model of size-resolved aerosol microphysics: I. Model development and prediction of aerosol properties, Atmos. Chem. Phys., 5, 2227–2252, 2005a.

Spracklen, D. V, Pringle, K. J., Carslaw, K. S., Chipperfield, M. P. and Mann, G. W.: A global off-line model of size-resolved aerosol microphysics: II. Identification of key uncertainties, Atmos. Chem. Phys., 5, 3233–3250, 2005b.

Spracklen, D. V, Carslaw, K. S., Kulmala, M., Kerminen, V. M., Sihto, S. L., Riipinen, I., Merikanto, J., Mann, G. W., Chipperfield, M. P., Wiedensohler, A., Birmili, W. and Lihavainen, H.: Contribution of

particle formation to global cloud condensation nuclei concentrations, Geophys. Res. Lett., 35(6), D06808, doi:10.1029/2007GL033038, 2008.

Spracklen, D. V., Carslaw, K. S., Pöschl, U., Rap, A. and Forster, P. M.: Global cloud condensation nuclei influenced by carbonaceous combustion aerosol, Atmos. Chem. Phys., 11(17), 9067–9087, doi:10.5194/acp-11-9067-2011, 2011.

Stevens, R. G. and Pierce, J. R.: The contribution of plume-scale nucleation to global and regional aerosol and CCN concentrations: evaluation and sensitivity to emissions changes, Atmos. Chem. Phys. Discuss., 14, 21473-21521, doi:10.5194/acpd-14-21473-2014, 2014.

Tost, H., Jockel, P., Kerkweg, A., Sander, R., and Lelieveld, J.: Technical note: A new comprehensive SCAVenging submodel for global atmospheric chemistry models, Atmos.
Chem. Phys., 6, 565–574, 2006, http://www.atmos-chemphys.net/6/565/2006/.

Trivitayanurak, W., Adams, P. J., Spracklen, D. V and Carslaw, K. S.: Tropospheric aerosol microphysics simulation with assimilated meteorology: model description and intermodel comparison, Atmospheric Chemistry and Physics, 8(12), 3149–3168, 2008.

Twomey, S.: Pollution and the Planetary Albedo, Atmos. Environ., 8, 1251–1256, 1974.

Vehkamäki, H., Kulmala, M., Napari, I., Lehtinen, K. E. J., Timmreck, C., Noppel, M. and Laaksonen, A.: An improved parameterization for sulfuric acid-water nucleation rates for tropospheric and stratospheric conditions, J. Geophys. Res., 107(D22), 4610–4622, 2002.

Wang, P. K., Grover, S. N., and Pruppacher, H. R.: On the effect of electric charges on the scavenging of aerosol particles by clouds and small raindrops, J. Atmos. Sci., 35, 1735–1743, 1978.

Wang, M. and Penner, J. E.: Aerosol indirect forcing in a global model with particle nucleation, Atmos. Chem. Phys., 9(1), 239–260, doi:10.5194/acp-9-239-2009, 2009.

Wang, X., Zhang, L., and Moran, M. D.:Development of a new semi-empirical parameterization for below-cloud scavenging of size-resolved aerosol particles by both rain and snow, Geosci. Model Dev., 7, 799-819, doi:10.5194/gmd-7-799-2014, 2014.

Westervelt, D. M., Pierce, J. R., Riipinen, I., Trivitayanurak, W., Hamed, A., Kulmala, M., Laaksonen, A., Decesari, S. and Adams, P. J.: Formation and growth of nucleated particles into cloud condensation nuclei: model–measurement comparison, Atmos. Chem. Phys., 13(15), 7645–7663, doi:10.5194/acp-13-7645-2013, 2013.

Westervelt, D. M., Pierce, J. R., and Adams, P. J.: Analysis of feedbacks between nucleation rate, survival probability and cloud condensation nuclei formation, Atmos. Chem. Phys., 14, 5577-5597, doi:10.5194/acp-14-5577-2014, 2014.

Yu, F. and Luo, G.: Simulation of particle size distribution with a global aerosol model: contribution of nucleation to aerosol and CCN number concentrations, Atmos. Chem. Phys. Discuss., 9, 10597–10645, doi:10.5194/acpd-9-10597-2009, 2009.

Yu, F.: A secondary organic aerosol formation model considering successive oxidation aging and kinetic condensation of organic compounds: Global scale implications, Atmos. Chem. Phys., 11, 1083–1099, doi:10.5194/acp-11-1083-2011, 2011.

Zhang, L., Wang, X., Moran, M. D., and Feng, J.: Review and uncertainty assessment of size-resolved scavenging coefficient formulations for below-cloud snow scavenging of atmospheric aerosols, Atmos. Chem. Phys., 13, 10005–10025, doi:10.5194/acp-13-10005-2013, 2013.

Table 1. Summary of simulations

Simulation name	Interstitial coagulation	Critical diameter for activation	Assumed droplet diameter	Minimum temperature for use of revised coagulation
BASE	No	N/A	N/A	N/A
INT_65nm_10μm_238K	Yes	65 nm	10 μm	238 K
INT_65nm_13μm_238K	Yes	65 nm	13 μm	238 K
INT_40nm_10μm_238K	Yes	40 nm	10 μm	238 K
INT_65nm_10μm_258K	Yes	65 nm	10 μm	258 K

Table 2. Summary of the global mean change in aersosol number (N10 and N80) and the radiative effect for all sensitivity simulations versus the base case.

Simulation name	N10 2 km (new-BASE)	N80 2 km (new-BASE)	AIE (new-BASE)	
INT_65nm_10μm_238K	-18.4%	-10.2%	+1.02 W m^{-2}	
INT_65nm_13μm_238K	-20.8%	-11.7%	+1.18 W m^{-2}	
INT_40nm_10μm_238K	-21.3%	-10.9%	+1.25 W m^{-2}	
INT_65nm_10μm_258K	-15.0%	-10.5%	+0.48 W m^{-2}	

Table 3. Statistical summary of the comparisons of simulated to measured N10, N40, N80 and N150 across the 21 sites. Included statistics are log-mean bias (LMB), slope (m), and coefficient of determination (R^2). Bold font indicates the simulation performing best for each statistic.

Simulation	LMB				*m*				R^2			
	N10	N40	N80	N150	N10	N40	N80	N150	N10	N40	N80	N150
BASE	0.077	**-0.01**	**0.027**	0.046	0.77	0.83	0.82	**0.86**	**0.79**	0.82	0.80	0.74
INT_65nm_10µm_238K	-0.034	-0.101	-0.043	0.015	0.86	0.90	0.86	**0.86**	**0.79**	0.82	**0.81**	0.75
INT_40nm_10µm_238K	-0.053	-0.107	-0.041	0.015	0.85	0.89	0.86	**0.86**	**0.79**	0.82	**0.81**	0.75
INT_65nm_10µm_258K	**-0.022**	-0.09	-0.035	0.019	0.82	0.87	0.85	**0.86**	**0.79**	**0.83**	**0.81**	0.75
INT_65nm_13µm_238K	-0.05	-0.114	-0.054	**0.010**	**0.87**	**0.91**	**0.87**	**0.86**	0.78	0.82	**0.81**	**0.76**

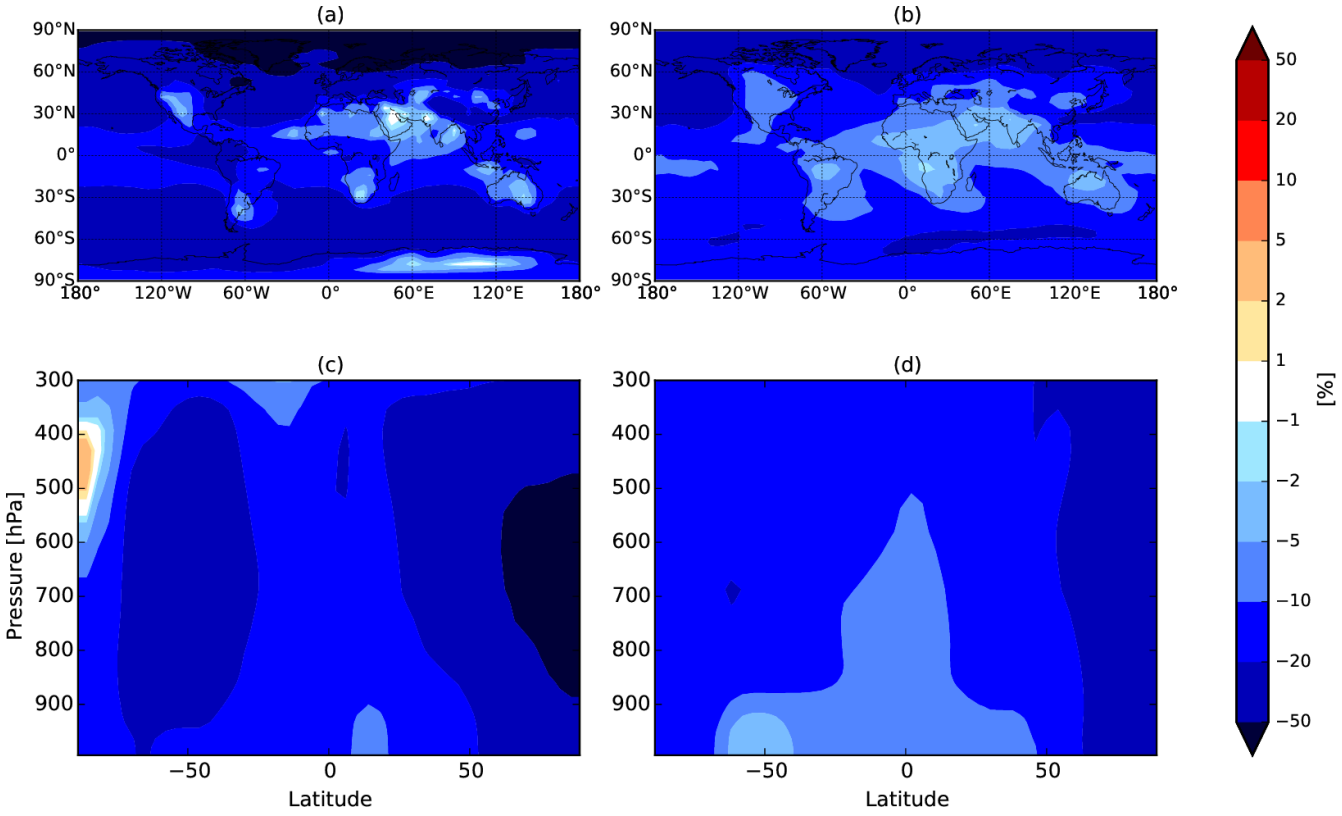

Figure 1. Annual-mean percent changes in N10 (panels a and c) and N80 (panels b and d) changes between INT_80nm_10µm_238K and BASE. Panels a and b show the changes for the 2 km model layer (representative of low clouds), and panels c and d show the zonal-mean changes throughout the troposphere.

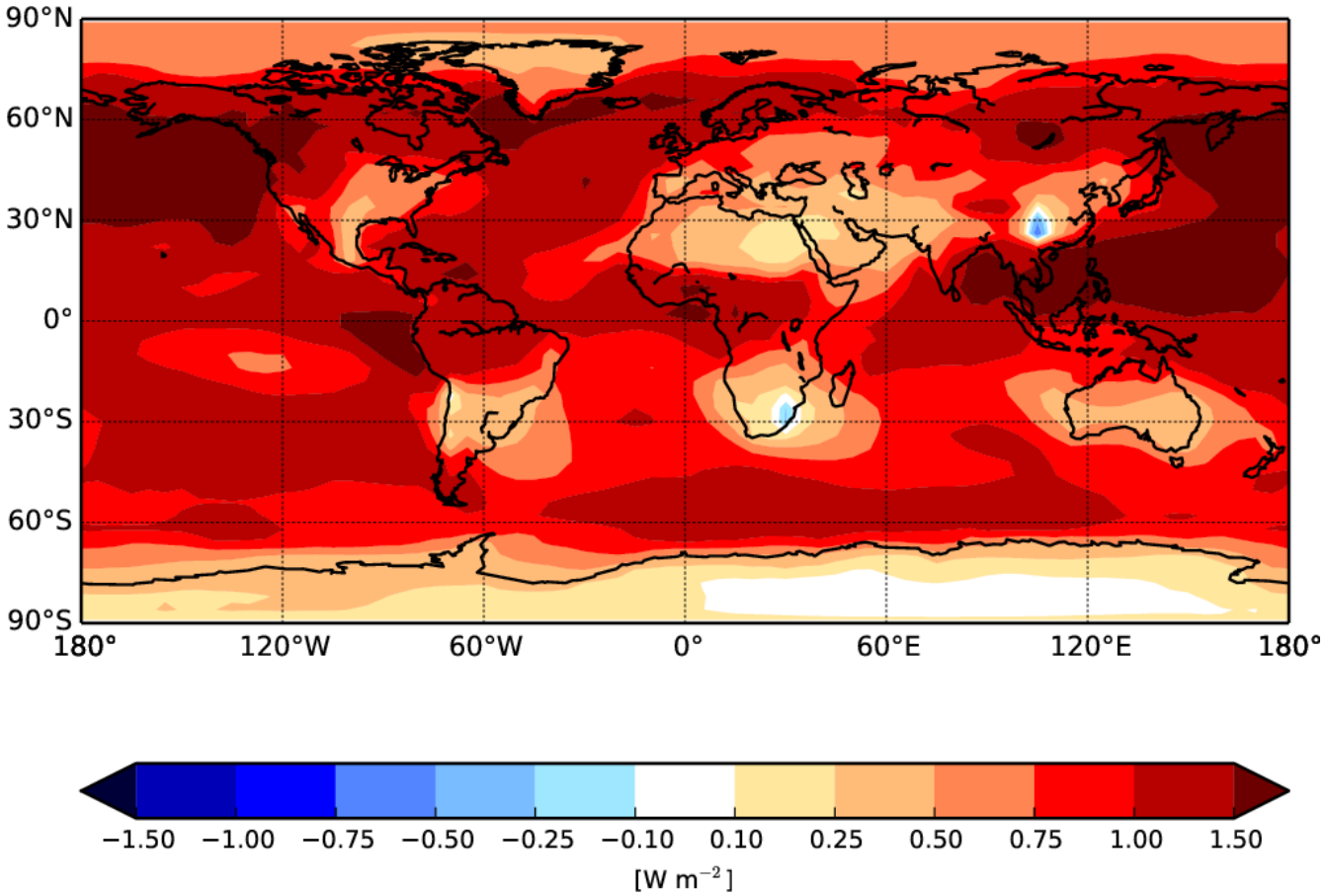

Figure 2. Annual-mean AIE between the INT_65nm_10μm_238K and the BASE simulation.

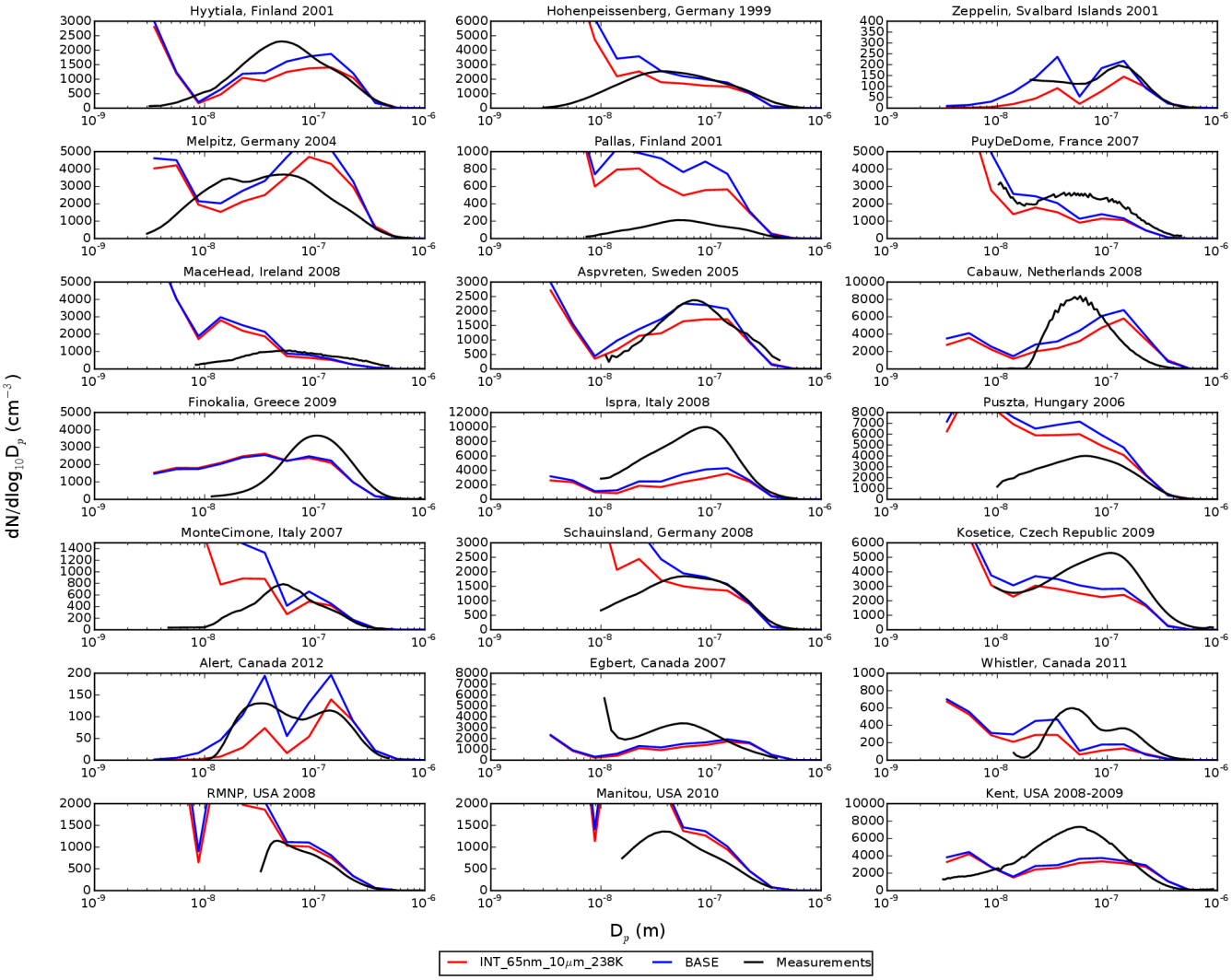

Figure 3. Observed and simulated (BASE and INT_65nm_10μm_238K) annual-mean aerosol number size distributions described in D'Andrea et al. (2013).

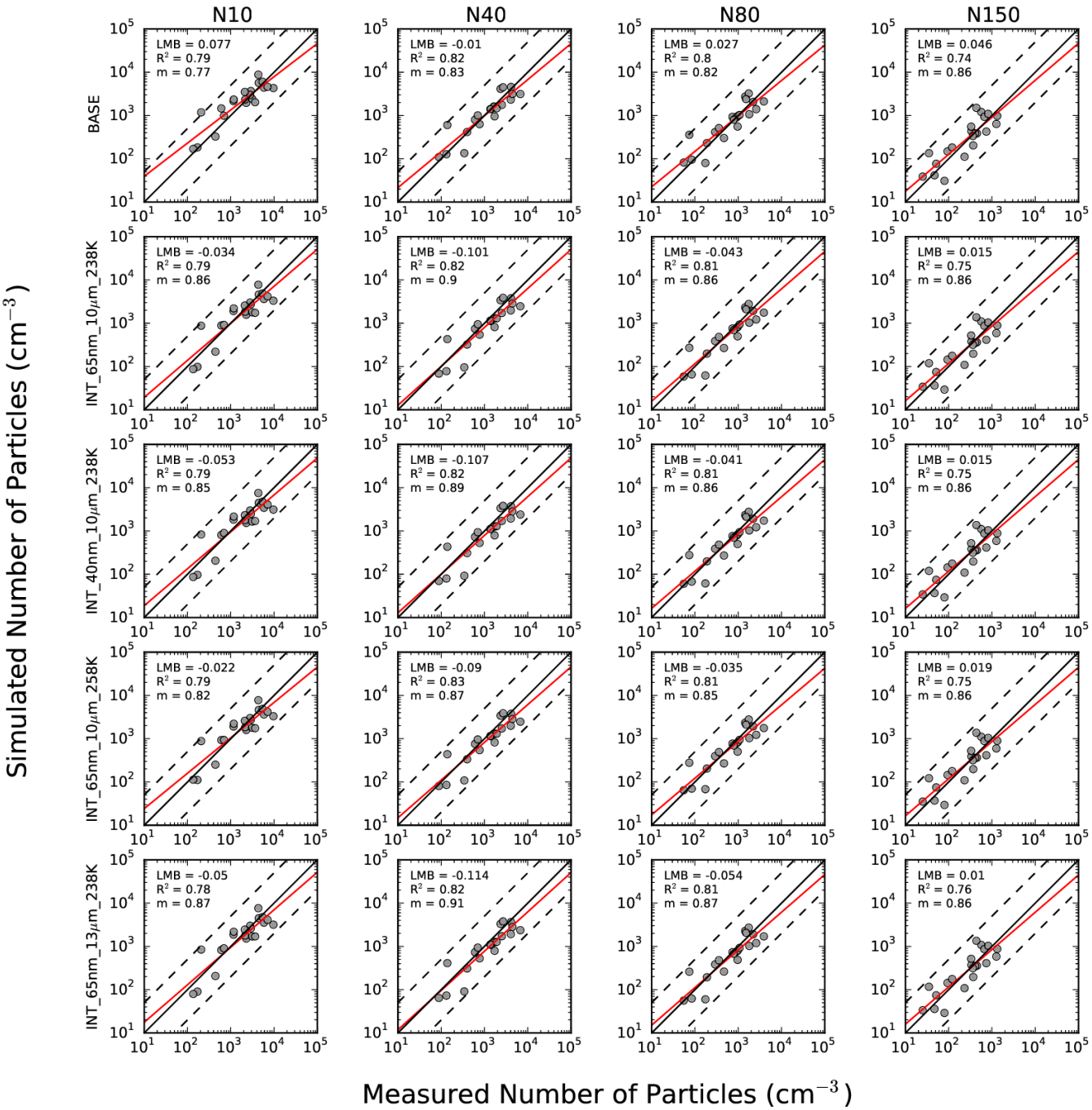

Figure 43. Annual-mean N10, N40, N80 and N150 GEOS-Chem-TOMAS simulation-to-measurement comparisons for the 5 simulations at the 21 SMPS measurement sites.